Articles

Sequence-Specific ^{1}H NMR Assignment and Secondary Structure of Neuropeptide Y in Aqueous Solution

Vladimir Saudek and John T. Pelton*

Merrell Dow Research Institute, 16 rue d'Ankara, 67084 Strasbourg, France

Received November 3, 1989; Revised Manuscript Received January 16, 1990

ABSTRACT: Sequence-specific assignment of the ^{1}H NMR spectrum of the 36 amino acid polypeptide porcine neuropeptide Y (pNPY) at pH 3.1 is reported. It was achieved by use of standard two-dimensional techniques and by a combination of the sequential and main-chain-directed assignment strategies. The secondary structure was derived from inspection of the nuclear Overhauser spectra, slow hydrogen–deuterium exchange effects, chemical shifts of main-chain HA resonances, and coupling constants. These studies indicate that the C-terminal segment (residues 11–36) folds into an amphiphilic α-helix; the N-terminal segment, containing three prolines in both cis and trans conformations, assumes no regular structure. CD studies of pNPY at pH 3.1 and 7.4 show an increase in ordered structure at neutral pH. The difference spectrum, however, is typical of an α-helix and suggests a stabilization of residues 11–36, possibly via Maxfield–Scheraga pair interactions involving side-chain residues. This is supported by a comparison of the one-dimensional ^{1}H NMR spectra of pNPY at pH 3.1 and 7.4, where no remarkable differences are observed.

Neuropeptide Y (NPY)[1] is a 36 amino acid peptide first isolated from porcine brain (Tatemoto et al., 1982) but since found to be widely distributed throughout the central and peripheral nervous systems of many mammalian species including man (Allen et al., 1983; Adrian et al., 1983). NPY derives its name from the presence of five tyrosine (Y) residues in the peptide, including tyrosine as the amino terminus and at the C-terminal amide position. NPY has considerable sequence homology with a family of pancreatic polypeptides (Table I). Indeed, it now appears that there are at least three members of the pancreatic polypeptide family within mammalian species (Allen & Bloom, 1986): NPY is found in cells derived from the neural crest; peptide YY is located only in gastrointestinal and pancreatic endocrine cells; pancreatic polypeptide (PP) is limited to pancreatic islets.

NPY is colocated with noradrenaline in many neurons of the sympathetic nervous system and is thought to be involved in the control of the cardiovascular system (Lundberg et al., 1982; Everitt et al., 1984). In vivo administration of NPY results in vasoconstriction and reduced heart rate and an overall increase in arterial blood pressure. The vasoconstriction observed with NPY has been found to be independent of adrenergic mechanisms and is antagonized by calcium channel blockers, both in vitro and in vivo.

Intracerebroventricular injection of NPY in conscious rats results in a large increase in both food intake and drinking via a mechanism that appears to be independent of a noradrenaline response (Stanley & Leibowitz, 1984). This has led to suggestions that NPY may be involved in feeding disorders. NPY may also play a role in certain degenerative diseases such as Alzheimer's (Allen et al., 1984).

Table I: Peptide Sequences of the Pancreatic Polypeptide Family[a]

	1 5 10 15 20 25 30 35
pNPY	YPSKP DNPGE DA PAE DLARY YSALR HYINL ITRQR Y
hNPY	YPSKP DNPGE DA PAE DMARY YSALR HYINL ITRQR Y
pPYY	YPAKP EAPGE DASP E ELSRY YASLR HYLNL VTRQR Y
aPP	GPSQP TYPGD DA PVE DLIRF YDNLQ QYLNV VTRHR Y

[a] pNPY, porcine neuropeptide Y; hNPY, human neuropeptide Y; pPYY, porcine peptide YY; aPP, avian pancreatic polypeptide.

Several studies have appeared recently that examine some of the biophysical properties of NPY in an attempt to better understand the molecular basis of its actions. Most of these studies are based, in part, on the sequence homology between NPY and avian pancreatic polypeptide (aPP), for which an X-ray analysis exists (Blundell et al., 1981). This model (Allen et al., 1987) predicts that NPY will assume a compact tertiary structure that is characterized by extensive hydrophobic interactions between the N-terminal polyproline-like helix and an α-helix that extends from residue 14 to about residue 30. This model is supported by CD studies (Krstenansky & Buck, 1987) in which a strong negative ellipticity at 222 nm, which is characteristic of α-helices (Chen et al., 1972), is observed and by molecular modeling studies in which the C-terminal region could adopt an amphipathic α-helix that facilitates hydrophobic interactions with the lipophilic residues of the polyproline helix. To better understand the solution structure of NPY, we have examined the ^{1}H NMR spectral properties of this peptide in water. In this paper, we present the complete sequence-specific assignment of the ^{1}H resonances and the secondary structure derived from the NMR and CD data.

[1] Abbreviations: NPY, neuropeptide Y; NMR, nuclear magnetic resonance; CD, circular dichroism; 2D, two dimensional; COSY, 2D correlated spectroscopy; HOHAHA, 2D homonuclear Hartmann–Hahn spectroscopy; NOE, nuclear Overhauser enhancement; NOESY, NOE 2D spectroscopy; ROESY, rotating-frame NOESY; $^3J_{HN-HA}$, coupling constant of HN and HA resonances; ppm, parts per million. The Brookhaven database notation is used for the hydrogens of the amino acids; e.g., HA, HB, etc. stand for CHα, CHβ, etc. An index identifies the position in the primary sequence; if no index is specified, all hydrogens belong to one residue.

0006-2960/90/0429-4509$02.50/0

Materials and Methods

Peptide Synthesis. Porcine NPY was synthesized by standard solid-phase synthetic techniques using an automated peptide synthesizer employing Boc/Bzl chemistry (Merrifield, 1963; Stewart & Young, 1984) and *p*-methylbenzhydrylamine–resin (0.49 mmol/g of resin). The peptide was deprotected and removed from the resin with the two-step "low–high" HF method (Tam et al., 1983) and purified by gel filtration, cation exchange chromatography, and preparative C_{18} reverse-phase HPLC. The purified peptide was characterized by analytical HPLC and TLC in two solvent systems. Amino acid analysis after acid hydrolysis gave the proper molar ratios (±8.0%) of the constituent amino acids: FAB–MS, MH^+ = 4252.4 (calcd = 4252.1).

Sample Preparation. Porcine NPY was dissolved in 0.05 M deuterioacetic acid in H_2O or D_2O. Concentrations were determined by UV absorbance (ϵ_{280nm} = 6724 M^{-1} cm^{-1}). Unless stated otherwise, the concentration was about 4 mM, pH 3.1. The reported pH is a direct meter reading with no correction for the isotope effect. The chemical shift was referred to the internal standard 3-(trimethylsilyl)propionic-d_4 acid.

Circular Dichroism. CD studies were performed with an Aviv Model 62D spectropolarimeter in D_2O at 37 °C at pH 3.1 or 7.4. Spectra were recorded with a 1.5-nm bandwidth, a 0.5-nm step, and a time constant of 4 s. A total of five scans were averaged for both sample and solvent. After correction of the sample spectrum for solvent contributions, the data were fit by nonlinear regression analysis. The CD spectrum for an ideal α-helix was computed as previously described (Chang et al., 1978). The instrument was calibrated with (+)-10-camphorsulfonic acid (Tuzimura et al., 1977). Circular cells with a 0.183-mm path length, measured by an infrared spectrometer (Bree & Lyons, 1956), were used.

NMR Spectroscopy. All spectra were acquired at 37 °C on a Bruker AM 500-MHz spectrometer equipped with an Aspect 3000 computer and a digital phase shifter. A set of standard (Wüthrich, 1986) 2D spectra was accumulated in the phase-sensitive mode (Redfield & Kunz, 1975; Marion & Wüthrich, 1983) with time proportional phase incrementation: COSY (Marion & Wüthrich, 1983), double quantum filtered COSY (Rance et al., 1983), NOESY (Jeener et al., 1979; Macura et al., 1981), HOHAHA (Bax & Davis, 1985; Rance, 1987), and ROESY (Bothner-By et al., 1984). In order to minimize any spin-diffusion effect, NOE buildup was followed in the NOESY spectra with mixing times of 100, 200, 300, 400, and 500 ms. Spin-locking experiments used a radio-frequency field strength between 5 and 7 kHz with mixing times of 18, 36, and 100 ms for HOHAHA and 100 and 300 ms for ROESY.

Solvent suppression was achieved by irradiation of the H_2O peak during the relaxation delay (1.5 s) and in NOESY experiments during the mixing time as well. Data were accumulated with 32 transients and 4 dummy transients in 2048 data points in the second time domain (t_2) and in 512 in the first one (t_1). The transmitter offset was placed on the H_2O resonance. A spectral width of 5 kHz and an incrementation in t_1 of 100 μs were applied. Data processing took place off-line on a Bruker station X32, using the manufacturer's program UXNMR. Prior to Fourier transformation the free induction decays were multiplied with a Gaussian or a shifted sine-bell weighting function and a cosine-bell function in t_2 and t_1, respectively. Zero-filling led to digital resolution of 2.44 and 4.88 Hz/point in the second (F_2) and first (F_1) frequency domains, respectively. The base line was fitted with a third-degree polynomial in both directions and subtracted from the spectra. The horizontal and vertical axes of the spectra in the figures represent F_2 and F_1, respectively. The contour levels are spaced logarithmically, and no symmetrization was applied.

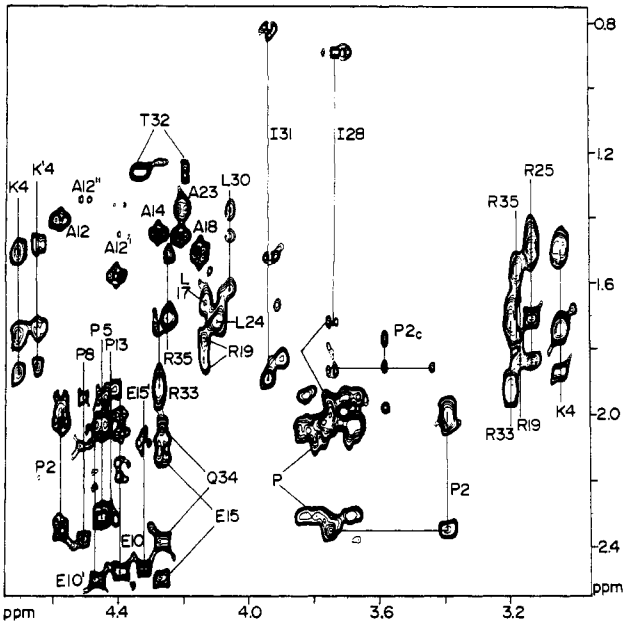

FIGURE 1: Part of the aliphatic region of the HOHAHA spectrum of NPY (mixing time 100 ms) in D_2O. Cross-peaks of HAs of several residues, HDs of prolines and arginines, and DE of lysine are labeled with the residue symbols. In this and the following figures, subscript c on t relates to the cis or trans conformation of a proline or the nearest proline in the sequence. If a residue provided several peaks due to the cis or trans conformation of a sequentially remote proline, the peaks are labeled with primes. If primes and subscripts are omitted, the trans conformation is implied. P indicates unresolved HD/HB and HD/HG cross-peaks of prolines.

Results and Discussion

Assignment Strategy. Porcine NPY consists of 36 amino acids, yet inspection of the 2D spectra reveals a larger number of cross-peaks than one would expect for a 36-spin system. This can be immediately seen in the HA/HB and HN/HA regions and elsewhere, such as the aromatic region which contains six cross-peaks for five tyrosines or the HA region in Figure 1 where two spin system cross-peaks are observed for one lysine. This indicates the existence of multiple conformations. Moreover, the majority of the cross-peaks are squeezed into a narrow region of 0.5 ppm, in both the HN and HA regions. Consequently, some of the HA/HN cross-peaks in the fingerprint part of the COSY spectrum could not be resolved into their individual resonances. In order to overcome this complication, we combined the standard sequential procedure (Wüthrich, 1986) with the main-chain-directed strategy (Englander & Wand, 1987). We first assigned most of the spin systems in the COSY and HOHAHA spectra, delineated the regular secondary structure NOE pattern, identified the assigned spin systems in this pattern, and completed the assignment of the irregular sequences by the standard sequential assignment method.

Spin System Identification. Alanines, threonine, leucine, isoleucines, glutamine/glutamic acids, asparagines/aspartic acids, and serines were recognized by their chemical shifts and COSY and HOHAHA (e.g., Figure 1) connectivity patterns (Wüthrich, 1986). Glutamine and the asparagines were distinguished from the corresponding acids according the HB/HG and HG/HD NOESY cross-peaks, respectively. Tyrosines were identified according to their COSY and

Table II: Summary of NOEs Used for the Sequential Assignment[a]

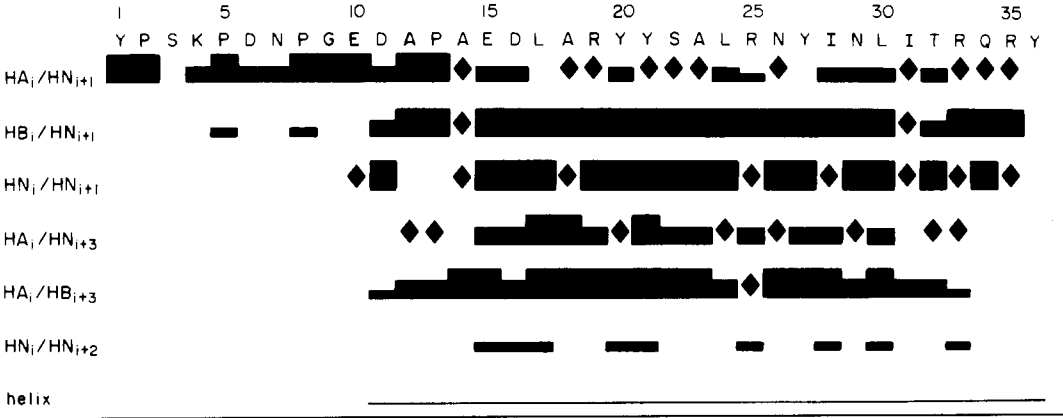

[a] The height of the bars reflects the intensities in the NOESY spectrum (200-ms mixing time). For the residues preceding the prolines, HA$_i$/HD$_{i+1}$ instead of HA$_i$/HN$_{i+1}$ is given. The symbol (◆) means that the NOE could not be detected because it was obscured by a stronger one or that the chemical shifts of the two resonances involved were nearly identical. The line indicates the residues in a helical conformation.

HOHAHA HD/HE and NOESY HD/HB and HD/HA cross-peaks. Histidine was assigned similarly according to HE1/HE2 and HE1/HB and HE1/HA cross-peaks. Glycine gave a typical cross-peak with large geminal coupling and two HA/HN cross-peaks in NOESY spectra. Arginines and lysine were first identified via the HE or HZ cross-peaks, respectively, with the remaining resonances in the H_2O HOHAHA spectrum. Alignment of these resonances with those in the D_2O HOHAHA spectrum allowed assignment of the two spin systems. Arginines, tyrosines, and histidine were localized in the H_2O NOESY spectrum from their respective HE/HN, HD/HN, and HE2/HN cross-peaks.

Prolines in the trans conformation were identified first with the aid of sequential NOESY cross-peaks HA$_{i-1}$/HD$_i$, and then the entire spin system was delineated in the HOHAHA spectrum. Cis forms provided one sequential HA$_{i-1}$/HA$_i$ NOESY cross-peak. Additionally, the slow exchange between cis and trans conformations detected in the ROESY (Figure 2) and NOESY spectra made it possible to locate the amino acid preceding *cis*-prolines in the sequence. In the case of the sequence Y1-P2, where the difference in the chemical shift of the HD resonances of the cis and trans conformation was large, the cis/trans exchange cross-peak of the HD resonance was detected as well (Figure 2).

Main-chain-directed sequential assignment (Englander & Wand, 1987) is based on the fact that different types of regular secondary structure of a protein provide different and characteristic regular patterns in the NOESY spectrum. Their delineation may be achieved prior to sequential assignment and leads immediately to the assignment of the main-chain resonances. Secondary structure prediction (Chou & Fasman, 1977) and CD studies (Krstenansky & Buck, 1987) indicate the presence of a helical conformation in pNPY. The typical helical NOE pattern has been summarized (Saudek et al., 1989a), and all its characteristic NOE connectivities are listed in the headings of Table II. Most of these connectivities can indeed be found for a long sequence in pNPY. Figure 3 shows HN$_i$/HN$_{i+1}$ cross-peaks arranged in a sequence. The corresponding HOHAHA spectrum of the amide region provided HA/HN cross-peaks which were then identified in the NOESY spectrum and aligned with the HB$_i$/HN$_{i+1}$ cross-peaks. These sequential connectivities confirm the sequential arrangement of the HN$_i$/HN$_{i+1}$ cross-peaks in Figure 3. The typical helical HA$_i$/HB$_{i+3}$ NOEs are also shown in Figure 4. Some additional weaker helical NOEs are listed in Table II. The identified HA and HB resonances in the helical NOE

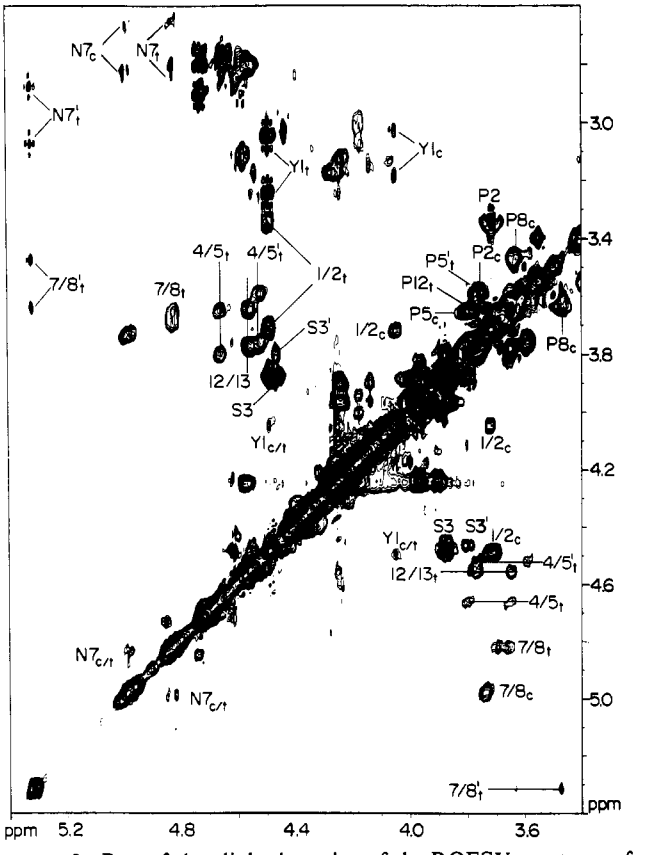

FIGURE 2: Part of the aliphatic region of the ROESY spectrum of NPY (mixing time 300 ms) in D_2O illustrating the cis/trans conformational equilibrium of the prolines. Positive and negative values are plotted without distinction (the exchange peaks are positive). The proline sequential peaks HA$_i$/HD$_{i+1}$ and HA$_i$/HA$_{i+1}$ (negative) are labeled with the sequence numbers. The exchange peaks between the cis and trans conformations are labeled with the subscripts c/t. For other symbols, see Figure 1.

pattern enabled us to connect the previously identified spin systems with the main-chain resonances and obtain a full sequential assignment for this region (Table III). Note that the helical sequence contains one proline (P13), for which no cis conformation was detected.

N-Terminus. Assignment of the individual prolines residues gave immediately the assignment of the preceding residues (Figure 2). These two-residue segments were joined via HA$_i$/HN$_{i+1}$ connectivities (Table II) and provided a full sequential assignment of pNPY. Table III lists the complete

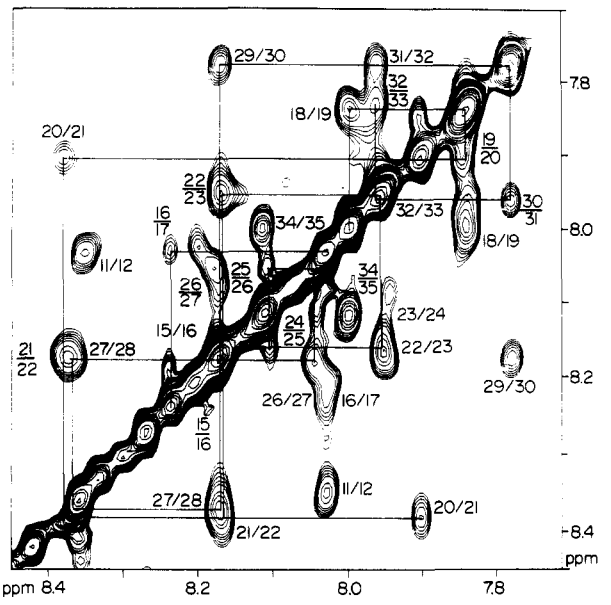

FIGURE 3: Diagonal part of the HN region of the NOESY spectrum (mixing time 200 ms) of NPY in H_2O showing HN_i/HN_j cross-peaks between residues 11–35 labeled with the sequence numbers of the two residues involved. The sequence was found to fold in a helix. The lines indicate the sequential arrangement of the peaks. NOEs 21/22 and 27/28 were resolved at 32 °C with a stronger resolution enhancement.

assignment for the trans conformation; the assignment of the cis conformation is shown in Figure 2.

Origin of Multiple Peaks. The first three prolines were found in both cis and trans conformations (Figure 2). This results in a different chemical environment, and thus a different chemical shift, for the residue preceding each such proline. These different conformations give rise to additional splitting of some resonances associated with residues further removed in the sequence. This is best illustrated by the case of N7 in the sequence P5-D6-N7-P8: due to the low-field chemical shift of HA in N7, its cross-peaks are located in a very clear part of the spectrum (Figure 2), and four different conformations of N7 may be detected. According to the integral intensities in the one-dimensional spectrum, pNPY contains N7 surrounded by 50% trans–trans, 27.5% cis–trans and trans–cis, and 22.5% cis–cis conformations of the two prolines in the sequence P5-D6-N7-P8. In this way, all peaks detected in the 2D spectra and not listed in Table III were assigned (as indicated in Figures 1 and 2), although it was not possible to determine which conformation of the more sequentially remote prolines was associated with the individual resonances.

Hydrogen Exchange. The resistance of an amide proton to exchange with deuterons in D_2O is an indication of hydrogen bonding and/or low accessibility to the solvent (Wüthrich, 1986). HNs of the following residues were found to exchange slowly in D_2O: L17, A18, Y20, Y21, L24, I28, L30, I31, and T32. They were assigned in a one-dimensional spectrum 1 h after dissolution of the sample in D_2O, although they were detectable for at least 12 h. However, they could not be unequivocally identified in two-dimensional spectra. The prolonged stability cannot be due solely to the chemical induction effects (Molday et al., 1972), and we interpret it as an indication of hydrogen bonding. Note that all stable hydrogens cluster in one region of the secondary structure (see discussion below).

Secondary Chemical Shift. The chemical shift of the HA resonance is sensitive to the dihedral angle W between HA and the carbonyl (Clayden & Williams, 1982). If no other

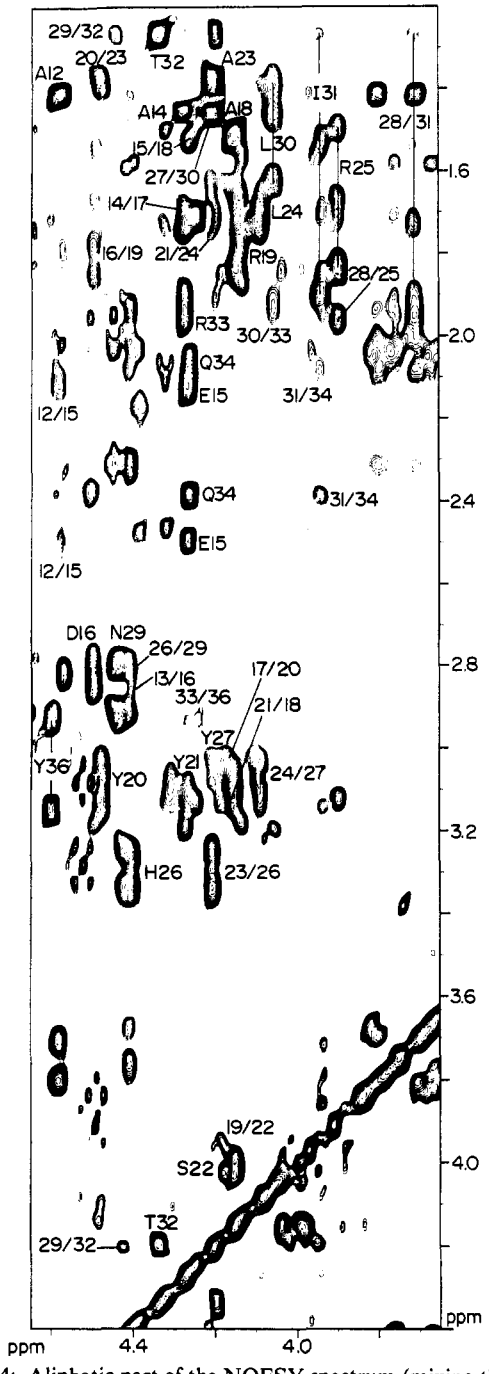

FIGURE 4: Aliphatic part of the NOESY spectrum (mixing time 200 ms) of NPY in D_2O showing the typical medium-range NOEs in the sequential distance $i,i+3$. The intraresidue cross-peaks of HA are labeled with the residue symbols, and the helical connectivities HA_i/HB_{i+3} and HA_i/HG_{i+3} are identified with the sequence numbers of the two residues involved. NOEs 26/29 and 13/16 appeared resolved clearly at 32 °C.

effects intervene, the helical conformation leads to an up-field shift of the HA resonance, as compared to that of the random coil (Dalgarno et al., 1983). Figure 5a shows that most of the HA resonances of pNPY are indeed shifted up field for the helical segment. As with other proteins (Saudek et al., 1989b) the trend is especially clear if an averaging is applied (Figure 5b).

Coupling Constants. The $^3J_{HN-HA}$ coupling constant between HA and HN hydrogen resonances could be assessed by cross sections through HA/HN COSY cross-peaks in the F_2 dimension for residues in the N-terminal segment (except for Y1 and, of course, for the prolines). Their values were found to be 9–8 Hz. This approach was not practicable for the helical

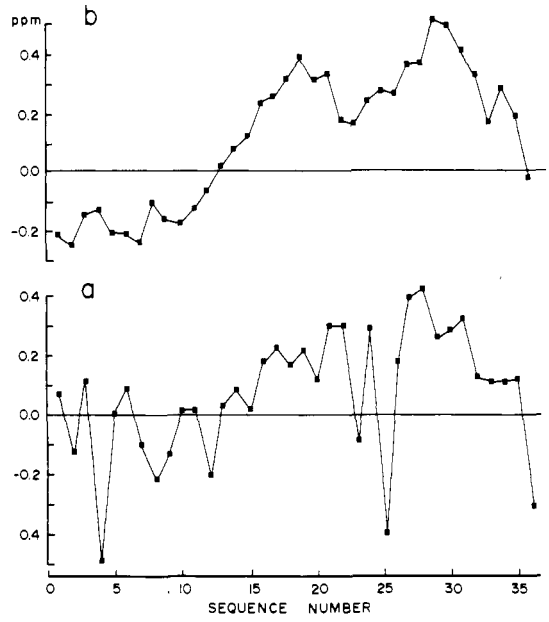

FIGURE 5: Secondary chemical shift of HA resonances [defined as the difference between the measured value (Table III) and that of peptide amino acid in the random coil conformation (Wüthrich, 1986)] plotted versus the sequence: (a) direct plot; (b) averaged values (for each residue, its value together with the values of one preceding and one succeeding residue were averaged).

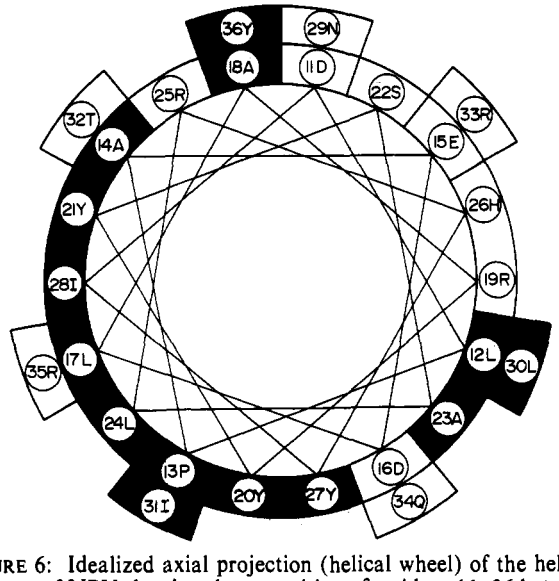

FIGURE 6: Idealized axial projection (helical wheel) of the helical segment of NPY showing the repartition of residues 11–36 between hydrophobic (black) and hydrophilic faces.

segment as the COSY peaks were not sufficiently resolved. Some $^3J_{HN-HA}$ of ≤4 Hz were estimated in a one-dimensional spectrum of a sample freshly dissolved in D_2O, where only slowly exchanging HNs remained.

Secondary Structure. The assignment procedure revealed the presence of a long α-helical region from residues 11 to 36. In addition to the NOEs in Table II, many NOEs involving side chain–side chain interactions were detected (about three to five NOEs per residue), confirming a helical conformation. All slowly exchanging HNs that could be detected were located within this segment, indicating the presence of hydrogen bonds. All slowly exchanging HNs belong to hydrophobic residues and are located on one side of the helix (Figure 6). Further indications of a helical conformation are the up-field shifts of the HA resonances (Figure 5) and, where measurable, the $^3J_{HN-HA}$ coupling constants of about 4 Hz (torsion angle $\phi \sim 60°$; Pardi et al., 1984). Note that the helical sequence con-

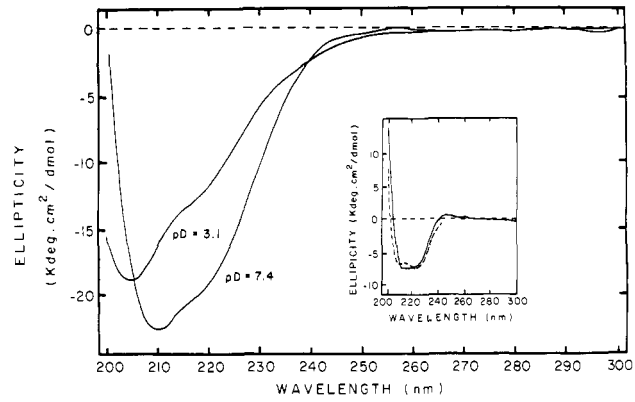

FIGURE 7: CD spectra of pNPY in D_2O. The CD spectrum at pD 7.4 shows an increase in secondary structure relative to that at pD 3.1. Inset: (solid curve) difference spectrum, pD 7.4 minus pD 3.1; (dashed curve) calculated spectrum of an ideal α-helix.

tains one proline (P13). This is the only proline for which no cis conformation was detected. The helical fold apparently stabilizes the trans conformation. As observed previously with proteins (Richardson & Richardson, 1988), proline may occupy one of the three peripheral positions of a helix, and because it cannot participate in the hydrogen bonding, it disrupts extension of the helix. Thus in pNPY the residue that cannot be hydrogen bonded in the helix is at position 10, and the helix is initiated by residue 11.

In contrast to the C-terminal segment 11–36, the N-terminus revealed no sign of any regular structure, and no nonsequential NOEs were detected. The chemical shifts of the HA protons are close to those of a random coil (Figure 5), no slowly exchanging NHs were detected, and the $^3J_{HN-HA} >$ 8 Hz coupling constants are characteristic for extended conformations ($\phi \sim 120°$). All three prolines in this sequence exchange between cis and trans conformations. This multiple conformational equilibrium is typical for small mobile peptides (Dyson et al., 1988) but has also been found in proteins (Chazin et al., 1989).

Our study has been performed at pH 3.1. The peptide could not be investigated by 2D methods at neutral pH because of its much lower solubility under these conditions (about 0.1 mM). However, no significant differences were observed when the one-dimensional spectra at pH 3.1 and 7.4 were compared. There is, for instance, no observable change in the aromatic region of the tyrosines. The CD spectra of pNPY at pH 3.1 and 7.4 are shown in Figure 7. The spectra are characterized by negative absorptions at 222 nm (shoulder) and 210 nm and a positive absorption at about 190 nm, the latter not shown. Such a profile is characteristic of an α-helix. Methods for estimating the length of the helix from the $n\pi^*$ rotational strength in the CD near 220 nm have been published (Chen et al., 1972). However, application of these methods to peptides is made difficult by the lack of experimental studies of end effects (Goodman et al., 1969). The situation is further complicated by the relatively large fraction (16%) of aromatic residues within the putative helical region of pNPY. The interaction of amide and aromatic transitions is known to strongly perturb the CD spectrum (Woody, 1977). Nevertheless, the negative $\pi\pi^*$ transition near 210 nm has been shown to be absent in short helices and appears only for chain lengths of 10 or more residues (Woody, 1985).

Most notable in the CD spectra is the increase in the ordered conformation at physiological pH, as previously reported (Krstenansky & Buck, 1987). The difference between the spectra at pH 3.1 and 7.4 is shown in the inset of Figure 7. The dashed line shows the calculated CD spectrum of an ideal

Table III: Proton Chemical Shifts of NPY in Aqueous Solution at 37 °C and pH 3.1

		chemical shift (ppm)								
residue no.	amino acid	HN	HA	HB		HG	HD		HE	others
1	Y		4.53	3.05	3.28	2.06	7.28		6.93	
2	P		4.59	2.01	2.39	1.48	3.38	3.74		
3	S	8.42	4.38	3.83						
4	K	8.27	4.72	1.74	1.83	1.48	1.48		3.03	NZ 7.52
5	P		4.45	2.33	1.97	2.02	3.63	3.82		
6	D	8.27	4.57	2.87	2.70					
7	N	8.47	4.82	2.63	2.79	6.88				
						7.55				
8	P		4.50	2.39	1.95	2.11	3.68	3.83		
9	G	8.49	3.97							
			4.29							
10	E	8.03	4.38	2.05	2.16	2.49				
11	D	8.37	4.76	2.95						
12	A	8.03	4.59	1.59						
13	P		4.42	2.32	1.95	2.00	3.51	3.80		
14	A	8.25	4.27	1.47						
15	E	8.25	4.28	2.08	2.12					
16	D	8.19	4.49	2.88		1.67				
17	L	8.03	4.14	1.76			0.95	0.88		
18	A	7.98	4.17	1.53						
19	R	7.85	4.15	1.65	1.82	1.51	3.18		7.14	HH 6.65
20	Y	7.88	4.48	3.05	3.52		6.95		6.77	
21	Y	8.37	4.28	3.07	3.17		7.10		6.80	
22	S	8.14	4.18	3.97	4.02					
23	A	7.95	4.21	1.42						
24	L	8.16	4.07	1.63		1.66	0.90	0.93		
25	R	8.08	3.85	1.82	1.63	1.52	3.12		7.18	HH 6.65
26	H	8.04	4.45	3.12	3.24					HE2 6.87
										HE1 8.63
27	Y	8.17	4.17	3.03	3.11		7.06		6.83	
28	I	8.36	3.77	1.92			0.84			HG1 1.58, 0.84; HG2 0.90
29	N	8.16	4.47	2.82	2.90	6.85				
						7.48				
30	L	7.77	4.08	1.66	1.43	1.50	0.79	0.72		
31	I	7.96	3.89	1.90			0.65			HG1 1.12, 1.58; HG2 0.84
32	T	7.97	4.35	4.20		1.26				
33	R	7.83	4.23	1.87	1.93	1.70	3.19		7.16	HH 6.65
34	Q	8.00	4.28	2.09	2.10	2.39	6.78	7.62		
35	R	8.10	4.27	1.63	1.72	1.50	3.20		7.11	HH 6.65
36	Y	8.00	4.61	2.82	3.14		7.15		6.85	
37	NH_2	7.42								

α-helix between 200 and 240 nm, and the close fit suggests that the newly formed structure at physiological pH is predominantly α-helical in nature. We can exclude the possibility that the increase in helical content is due to the formation of a polyproline-like helix in the proline-rich N-terminus, as the CD spectrum of such a helix (Carver et al., 1966; Young & Pysh, 1975) is very different from that in the inset of Figure 7. We suggest rather that the α-helix between residues 11–36 stabilizes at pH 7.4. It has been observed, for example, that charged, helical residues often have a neutralizing neighbor of opposite charge four residues away on the helix (Maxfield & Scheraga, 1975). Low pH could disrupt the ionic interaction of such Maxfield–Scheraga pairs as D16 and R19, which are brought together by the helical fold (Figure 6).

The helical NOEs detected are stronger in the middle of the helix than at the ends (Table II). Similarly, the greatest number of NOEs between the side chains was observed for the middle residues. These findings indicate that at pH 3.1 the helix is better defined for its central part, whereas its peripheral elements are less constrained. Again, such end effects may be responsible for some of the differences observed in the CD spectra. In addition, the slow exchange of the HNs of the hydrophobic residues, which are all located on one side of the helix, indicates enhanced stability of this face of the molecule. Many NOEs between the hydrophobic side chains were observed that cannot be explained solely by the helical fold. A preliminary analysis indicates that porcine pNPY, under our NMR conditions, probably exists as a dimer via interactions of the hydrophobic residues in the helical region. Such a dimeric arrangement is also observed in the crystal structure of the homologous avian pancreatic polypeptide, and a more detailed analysis of these NOEs is in progress.

Analysis of the line widths in the aromatic part of the one-dimensional spectrum of pNPY shows that both terminal tyrosines are more mobile than the three central ones. However, whereas Y1 does not show any interaction with the rest of the molecule, Y36, which has been found to be crucial for biological activity of this peptide, participates in the helix, and its side chain is located between T32 and Q34. Again, the dynamics of individual residues and a more detailed description of the three-dimensional structure are in progress.

An Edmundson wheel diagram of the helix between residues 11–36 is shown in Figure 6. The helix is clearly amphiphilic with only minor perturbation of the hydrophobic face. Similar arrangements have been observed in other biologically active helical peptides such as ACTH (Schwyzer, 1986), calcitonin (Moe & Kaiser, 1985), and melittin (Bazzo et al., 1988). Amphiphilicity has been found to be important for the biological activity of such peptides (Green et al., 1987), and its presence in pNPY may provide new insight into the activity of this molecule.

Conclusions

This study provides complete assignment of the ^1H NMR

spectrum of porcine NPY, and analysis of these data yields new insight into the secondary structure of this peptide. Our results indicate that the solution structure of pNPY is substantially different from the crystal structure of the homologous avian pancreatic polypeptide (Blundell et al., 1981) and thus from the structure of pNPY based on this model (Allen et al., 1987). The proline-rich N-terminus undertakes many different conformations due to the cis/trans isomerization of the prolines and prevents formation of any regular structure. While the crystal structure of avian pancreatic polypeptide would suggest a close association between the N-terminus and the hydrophobic part of the helix, in pNPY we oberve no contact between these two regions of the molecule. The most important secondary structural element is the helix. Its fold determines the orientation of the side chains, the distribution of the charges, and the creation of hydrophobic and hydrophilic faces. This study indicates that the helix encompasses residues 11–36, in contrast to residues 14–30 as suggested by analogy with avian pancreatic polypeptide. On the other hand, a dimeric arrangement of pNPY similar to that observed in the crystal structure of avian pancreatic polypeptide is probably preserved in solution as well.

ACKNOWLEDGMENTS

Part of the NMR experiments were done at the facilities of the Oxford Enzyme Group. We are indebted to Professor R. J. P. Williams for valuable discussions and for providing access to the spectrometer. We are grateful to Dr. Joseph Wagner for amino acid analysis and to Dr. Annalisa Pastore for preparation of Figure 5.

Registry No. Porcine neuropeptide Y, 83589-17-7; neuropeptide Y, 82785-45-3.

REFERENCES

Adrian, T. E., Allen, J. M., Bloom, S. R., Ghatei, M. A., Rossor, M. N., Roberts, G. W., Crow, T. J., Tatemoto, K., & Polak, J. M. (1983) *Nature 306*, 584–586.

Allen, J., Novotny, J., Martin, J., & Heinrich, G. (1987) *Proc. Natl. Acad. Sci. U.S.A. 84*, 2532–2536.

Allen, J. M., & Bloom, S. R. (1986) *Neurochem. Int. 8*, 1–8.

Allen, J. M., Ferrier, I. N., Roberts, G. W., Cross, A. J., Adrian, T. E., Crow, T. J., & Bloom, S. R. (1984) *J. Neurol. Sci. 64*, 325–331.

Allen, Y. S., Adrian, T. E., Allen, J. M., Tatemoto, K., Crow, T. J., Bloom, S. R., & Polak, J. M. (1983) *Science 221*, 877–879.

Bax, A., & Davis, D. G. (1985) *J. Magn. Reson. 65*, 355–366.

Bazzo, R., Tappin, M. J., Pastore, A., Harvey, T. S., Carver, J. A., & Campbell, I. D. (1988) *Eur. J. Biochem. 173*, 139–146.

Blundell, T. L., Pitts, J. E., Tickle, I. J., Wood, S. P., & Wu, C.-W. (1981) *Proc. Natl. Acad. Sci. U.S.A. 78*, 4175–4179.

Bothner-By, A. A., Stephens, R. L., Lee, J., Warren, C. D., & Jeanloz, R. W. (1984) *J. Am. Chem. Soc. 106*, 811–813.

Bree, A., & Lyons, L. E. (1956) *J. Chem. Soc.*, 2658–2670.

Carver, J. P., Schechter, E., & Blout, E. R. (1966) *J. Am. Chem. Soc. 88*, 2550–5103.

Chang, C. T., Wu, C.-S. C., & Yang, J. T. (1978) *Anal. Biochem. 91*, 13–31.

Chazin, W. J., Kördel, J., Drakenberg, T., Thulin, E., Brodin, P., Grundström, T., & Forsén, S. (1989) *Proc. Natl. Acad. Sci. U.S.A. 86*, 2195–2198.

Chen, Y.-H., Yang, J. T., & Martinez, H. M. (1972) *Biochemistry 11*, 4120–4131.

Chou, P. Y., & Fasman, G. D. (1977) *J. Mol. Biol. 115*, 135–175.

Clayden, N. J., & Williams, R. J. P. (1982) *J. Magn. Reson. 49*, 383–396.

Dalgarno, D. C., Levine, B. A., & Williams, R. J. P. (1983) *Biosci. Rep. 3*, 443–452.

Dyson, H. J., Rance, M., Houghten, R. A., Lerner, R. A., & Wright, P. E. (1988) *J. Mol. Biol. 201*, 161–200.

Englander, S. W., & Wand, A. J. (1987) *Biochemistry 26*, 5953–5958.

Everitt, B. J., Hokfelt, T., Terenius, L., Tatemoto, K., Mutt, V., & Goldstein, M. (1984) *Neuroscience 11*, 443–462.

Goodman, M., Verdini, A. S., Toniolo, C., Phillips, W. D., & Bovery, F. A. (1969) *Proc. Natl. Acad. Sci. U.S.A. 64*, 444–450.

Green, F. R., III, Lynch, B., & Kaiser, E. T. (1987) *Proc. Natl. Acad. Sci. U.S.A. 84*, 8340–8344.

Jeener, J., Meier, B. H., Bachmann, P., & Ernst, R. R. (1979) *J. Chem. Phys. 71*, 4546–4553.

Krstenansky, J. L., & Buck, S. H. (1987) *Neuropeptides 10*, 77–85.

Lundberg, J. M., Terenius, L., Hokfelt, T., Martling, C. R., Tatemoto, K., Mutt, V., Polak, J. M., Bloom, S. R., & Goldstein, M. (1982) *Acta Physiol. Scand. 116*, 477–480.

Macura, S., Huang, Y., Suter, D., & Ernst, R. R. (1981) *J. Magn. Reson. 43*, 259–281.

Marion, D., & Wüthrich, K. (1983) *Biochem. Biophys. Res. Commun. 113*, 967–974.

Maxfield, R. R., & Scheraga, H. A. (1975) *Macromolecules 8*, 491.

Merrifield, R. B. (1963) *J. Am. Chem. Soc. 85*, 2149–2154.

Moe, G. R., & Kaiser, E. T. (1985) *Biochemistry 24*, 1971–1976.

Molday, R. S., Englander, S. W., & Kallen, R. G. (1972) *Biochemistry 11*, 150–158.

Pardi, A., Billeter, M., & Wüthrich, K. (1984) *J. Mol. Biol. 180*, 741–751.

Rance, M. (1987) *J. Magn. Reson. 74*, 557–564.

Rance, M., Sorensen, O. W., Bodenhausen, G., Wagner, G., Ernst, R. R., & Wüthrich, K. (1983) *Biochem. Biophys. Res. Commun. 117*, 479–485.

Redfield, A. G., & Kunz, S. D. (1975) *J. Magn. Reson. 19*, 250–254.

Richardson, J. S., & Richardson, D. C. (1988) *Science 240*, 1648–1652.

Saudek, V., Atkinson, R. A., Williams, R. J. P., & Ramponi, G. (1989a) *J. Mol. Biol. 205*, 229–239.

Saudek, V., Williams, R. J. P., Stefani, M., & Ramponi, G. (1989b) *Eur. J. Biochem.* (in press).

Schwyzer, R. (1987) *EMBO J. 6*, 2255–2259.

Stanley, B. G., & Leibowitz, S. F. (1984) *Life Sci. 35*, 2635–2642.

Stewart, J. M., & Young, J. D. (1984) in *Solid Phase Peptide Synthesis*, Pierce Chemical Co., Rockford, IL.

Tam, J. P., Heath, W. F., & Merrifield, R. B. (1983) *J. Am. Chem. Soc. 105*, 6442–6455.

Tatemoto, K., Carlquist, M., & Mutt, V. (1982) *Nature 296*, 659–660.

Tuzimura, K., Konno, T., Meguro, H., Hatano, M., Murakami, T., Kashiwabara, K., Saito, K., Kondo, Y., & Suzuki, T. M. (1977) *Anal. Biochem. 81*, 167–174.

Woody, R. W. (1977) *Macromol. Rev. 12*, 181–321.

Woody, R. W. (1985) *Peptides 7*, 15–114.

Wüthrich, K. (1986) *NMR of Proteins and Nucleic Acids*, Wiley, New York.

Young, M. A., & Pysh, E. S. (1975) *J. Am. Chem. Soc. 97*, 5100–5103.